Loss of GABAB-mediated interhemispheric synaptic inhibition in stroke periphery

Bojana Kokinovic[1,2] and Paolo Medini[1] iD

[1] *Department of Integrative Medical Biology (IMB), Physiology section, Umeå University, Umeå, Sweden*
[2] *Department of Neuroscience and Brain Technologies (NBT), Italian Institute of Technology (IIT), Genova, Italy*
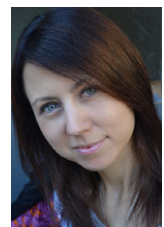
Edited by: Ole Paulsen & Diego Contreras

The Journal of Physiology

Key points

- Recovery from the potentially devastating consequences of stroke depends largely upon plastic changes occurring in the lesion periphery and its inputs.
- In a focal model of stroke in mouse somatosensory cortex, we found that the recovery of sensory responsiveness occurs at the level of synaptic inputs, without gross changes of the intrinsic electrical excitability of neurons, and also that recovered responses had longer than normal latencies.
- Under normal conditions, one somatosensory cortex inhibits the responsiveness of the other located in the opposite hemisphere (interhemispheric inhibition) via activation of GABAB receptors.
- In stroke-recovered animals, the powerful interhemispheric inhibition normally present in controls is lost in the lesion periphery.
- By contrast, contralateral hemisphere activation selective contributes to the recovery of sensory responsiveness after stroke.

Abstract Recovery after stroke is mediated by plastic changes largely occurring in the lesion periphery. However, little is known about the microcircuit changes underlying recovery, the extent to which perilesional plasticity occurs at synaptic input *vs.* spike output level, and the connectivity behind such synaptic plasticity. We combined intrinsic imaging with extracellular and intracellular recordings and pharmacological inactivation in a focal stroke in mouse somatosensory cortex (S1). *In vivo* whole-cell recordings in hindlimb S1 (hS1) showed synaptic responses also to forelimb stimulation in controls, and such responses were abolished by stroke in the neighbouring forelimb area (fS1), suggesting that, under normal conditions, they originate via horizontal connections from the neighbouring fS1. Synaptic and spike responses to forelimb stimulation in hS1 recovered to quasi-normal levels 2 weeks after stroke, without changes in

intrinsic excitability and hindlimb-evoked spike responses. Recovered synaptic responses had longer latencies, suggesting a long-range origin of the recovery, prompting us to investigate the role of callosal inputs in the recovery process. Contralesional S1 silencing unmasked significantly larger responses to both limbs in controls, a phenomenon that was not observed when $GABA_B$ receptors were antagonized in the recorded area. Conversely, such $GABA_B$-mediated interhemispheric inhibition was not detectable after stroke: callosal input silencing failed to change hindlimb responses, whereas it robustly reduced recovered forelimb responses. Thus, recovery of subthreshold responsiveness in the stroke periphery is accompanied by a loss of interhemispheric inhibition and this is a result of pathway-specific facilitatory action on the affected sensory response from the contralateral cortex.

Corresponding authors P. Medini & B. Kokinovic: Department of Integrative Medical Biology (IMB), Physiology section, Umeå University, 90187, Umeå, Sweden.   Email: paolo.medini@umu.se & bojana.kokinovic@umu.se

Introduction

Stroke is a leading cause of mortality and disability worldwide not only as a result of the loss of the affected neurons, but also because of functional deficits in their target areas. Neuroprotection strategies such as modulating NDMA receptors, anti-adhesion antibodies and membrane stabilization, as reviewed for example by Onwuekwe & Ezeala-Adikaibe (2012), aim to limit the halo of neuronal death around the core of the ischaemic area and are of some help in the (sub)acute time window after stroke. However, a significant degree of the recovery of the lost neurological function occurs over a longer time scale and is based on plastic changes of the brain connectivity that has the potential to take over the function at least partially (Silasi & Murphy, 2014). By contrast, stroke-associated plasticity can also contribute to additional clinical problems (e.g. hyperexcitability that might cause to post-stroke epilepsy and spasticity). Because opto-molecular tools that modify the activity of specific cell types are now available, it is important to fulfill our gap of knowledge about the precise microcircuit changes underlying stroke-induced plasticity. In that respect, a focal model of stroke is particularly useful because it allows the recovery process to be studied in the stroke vicinity (i.e. in an identified functional area), rendering more controlled and reproducible results. Indeed, the stroke outcome, as well as the vicariant mechanisms, are not only time-dependent (Biernaskie *et al.* 2004), but also dependent on lesion size, even within the same species (e.g. rodents).

One example of a reliable mouse focal stroke model uses both a voltage-sensitive dye (Brown *et al.* 2009) and calcium imaging (Winship & Murphy, 2008). This previous model shows that lesioning fS1 leads to a receptive field expansion of neurons in the neighbouring hS1 and to a subsequent cortical remapping. The experimental model also gives rises to detectable behavioural deficits (Brown *et al.* 2009) that go in parallel with the recovery of neuronal responses.

A largely debated issue on the circuit changes behind recovery is the degree to which any recovery is attributable to changes occurring in the lesion periphery *vs.* those occurring in distant cortical areas. In that respect, the role of the contralateral, healthy hemisphere remains controversial in part because it is both time- (Marshall *et al.* 2000) and size-dependent (Silasi & Murphy, 2014). Furthermore, direct electrophysiological measurements of the changes of synaptic strength of this connection after lesion are not available *in vivo*. Indeed, cortical map plasticity can be attributable to changes in either synaptic inputs (subthreshold plasticity) or in the action potential (AP) generating mechanisms (suprathreshold plasticity), as well as to a combination of these two types of plasticity. To address these issues, we used a combination of intracellular recordings from identified cells and extracellular recordings at different times after stoke, combined with acute callosal silencing experiments.

We found that the process of recovery of sensory responses in the stroke periphery occurs largely at the level of synaptic inputs without major changes in intrinsic cell excitability (AP generating mechanisms). Our data indicate that recovery from stroke is a result of the combined effect of the loss of the synaptic $GABA_B$-dependent inhibition between the two hemispheres observed in controls in the stroke periphery, as well as a pathway-specific facilitation of the recovered sensory response of callosal origin.

Methods

Ethical approval and animal procedures

Young male adult (postnatal day 30, weighing between 16 and 20 g) C57BL/6J mice (Charles River, Erkrath, Germany) were used. The animals were housed in the Umeå Centre for Comparative Biology's premises under a 12:12 h light/dark cycle and were provided with *ad libitum* access to food and water. All procedures were

conducted in accordance with the Ethical Committee of the Italian Institute of Technology, Genova, Italy, and the Swedish Ethical Committee for Northern Sweden (permit number A 44-13) and they conformed to the principles and regulations as described by Grundy (2015). All animal procedures and study design were performed in agreement with the ARRIVE guidelines for terminal experiments. Mice were anaesthetized with 20% urethane (0.8–1 g kg^{-1}) (I.P.). Anaesthesia depth was maintained on the surgical level during experiments with additional doses (5–10% of the initial dose). Anaesthesia depth was monitored by pinch and corneal reflexes, electrocardiogram and breathing rate. Before surgery, dexamethasone was injected (0.01 mg kg^{-1} I.M.) to prevent brain and mucosal oedemas and local anaesthetic (bupivacaine 2.5 mg mL^{-1}) was topically applied in the incision skin area. Humidified oxygen was administrated through a nose cannula, and the body temperature was held at 37°C. A metal recording chamber was placed onto the skull and fixed with acrylic glue and dental cement to allow intrinsic optical imaging (IOI) followed by electrophysiology [*in vivo* whole-cell recordings, local field potentials (LFPs)]. The region of the skull of interest was thinned by a dental drill until the vasculature underneath became visible. At the end of electrophysiological recordings, animals were killed with an I.P. bolus of urethane.

When IOI was used to induce stroke, mice were anaesthetized with ketamine 100 mg mL^{-1} + xylazine 20 mg mL^{-1}; 0.1 mL per 10 g of weight (I.P.). The animal head was secured to a stereotaxic apparatus and the skull was exposed without thinning to minimize invasiveness. Next, the small plastic imaging chamber was placed onto the exposed skull.

After surgery, the antibiotic steroid cream (Fucidin 2%; Leo Laboratories Limited, Maidenhead, UK) was applied along the surgical suture and pain killer was given (ketoprofen 5 mg kg^{-1}, I.M.). Then, the animal was placed on a heated pad and surveyed until it gained back full mobility and then left to recover in individual cages. Food softened with water was placed at the bottom of the cage after surgery. We carefully controlled physical (hydration, weight) and behavioural recovery from anaesthesia and from the procedure (Swedish Ethical Committee for Northern Sweden, permit number A 44-13).

IOI

Mapping the cortical representation of the forelimb and hindlimb area was performed by IOI as described previously (Iurilli *et al.* 2013). A vasculature image was acquired under 540 nm illumination before starting imaging. During IOI, the cortex was illuminated with monochromatic light of 630 nm. Images were acquired using a cooled 50 Hz CCD camera connected to a frame grabber (Imager 3001; Optical Imaging Ltd, Rabin Science Park, Israel) and defocused 500–600 μm below the pia. Data frame duration was 200 ms and a spatial binning of 3×3 was applied over the images, which were 4×4 mm. Stimulations of the limbs were achieved by touching the limbs with a sponge glued to a piezoelectric wafer (Physik Instrumente GmbH, Karlsruhe, Germany). Stimulation frequency was 100 Hz for 10 s, with a linear displacement of 2 mm. All image frames obtained during stimulus presentation were divided by the average image of the first 10 frames acquired just before stimulus presentation (Schuett *et al.* 2002). The relative decrease of reflectance, averaged over the stimulus presentation period, was then outlined. The spot area was taken as the area where the decrease in reflectance was 50% of the peak. This region was overlaid with the vasculature image.

Phototrombosis

To induce a focal stroke in fS1, we used the photo-thrombotic model (Brown *et al.* 2009; Takatsuru *et al.* 2009). Guided by the IOI functional cortical map, an optic fibre (NA 0.63, diameter 500 μm) was positioned on top of fS1. The area was illuminated with white light (11 mW, 15 min), 5 min after an I.P. injection of 1% Rose Bengal in physiological solution (100 mg kg^{-1}).

Electrophysiology

All the recordings were performed in hS1 as defined by IOI and the responses to both limbs were recorded. In the case of stroked animals, we took care to compare the hindlimb cortical representations as defined by IOI right before the stroke and at the time of recording and we also carefully checked to perform our recordings within the area of overlap between the pre-stroke and post-stroke hindlimb representation (Fig. 2*D*). This ensured that our electrophysiological recordings were performed in the same anatomo-functional region (i.e. compared to pre-stroke condition). We failed to observe major shifts of the hS1, in line with previous report showing that it is the representation of the stroked forelimb area that undergoes a major spatial shift (Brown *et al.* 2009).

***In vivo* whole cell recording.** Patch pipettes (5–8 MΩ) were filled with intracellular solution (in mM: 135 K-gluconate, 10 Hepes, 10 phosphocreatine-Na, 4 KCl, 4 ATP-Mg salt and 0,3 GTP, pH 7.2, osmolarity 291 mOsm) and lowered until layer 2/3 was reached (Margrie *et al.* 2002). Positive pressure (300–400 mbar) was applied before and also when lowering the pipette into the brain. Once the layer of interest was reached, the pressure was diminished to 30 mmHg to search for cells. Cells were searched in voltage clamp when advancing in 2 μm steps. When cells were approached, the pressure was

relieved, the pipette potential was hyperpolarized and light suction was applied to facilitate gigaseal formation. After compensation for electrode capacitance, usually a ramp of negative pressure led to whole-cell configuration. Recordings were performed with an EPC10 double plus amplifier (HEKA, Lambrecht, Germany) in voltage follower mode (current clamp) and the signal was digitized (20 kHz) and acquired with Patchmaster software (HEKA, Lambrecht, Germany).

Limbs were stimulated by computer-controlled movement of a piezoelectric wafer and by a single touch delivered 30 times every 5–7 s (on–off interval: 2000 ms; linear displacement: 2 mm).

Extracellular recordings. Glass pipettes (0.8–1.2 M Ω) filled with saline solution (0.9% NaCl) were inserted in layer 2/3 of mouse hS1. For LFP recordings, the signal was band-filtered (0.1–100 Hz) and amplified (1000×) with a DAM 50 differential amplifier (World Precision Instruments, Hitchin, UK). After reaching the area of interest, the two limbs were stimulated separately following the same stimulation protocol used for *in vivo* whole-cell recordings.

Analysis of cell excitability parameters and of the sensory responses

V_m values were calculated as the average membrane potential in the 200 ms time window before stimulus onset. The AP threshold was measured at the peak of the second derivative of the V_m trace (Wilent & Contreras, 2005). To analyse subthreshold responses, the sweeps were averaged after removal of the APs by linear interpolation. The time window for peak amplitude and latency calculations was 300 ms after stimulus onset. For analysis of the AP responses, spike counts were computed with 50 ms bins. An AP response was considered significant if, in the peri-stimulus time histogram, there was at least one bin that exceeded the mean + 2.5 SD spontaneous (prestimulus) firing frequency in a time window of 300 ms after stimulus onset. The peak AP response was taken as the highest firing frequency within that time window. For LFP response analysis, the peak amplitudes were relative to the average value of the first 200 ms pre-stimulus onset and the time window for peak search was also 0–300 ms poststimulus. For a grand average calculation of LFPs, the single averaged sweeps obtained from different animals were aligned so that the average voltage value of the prestimulus time was the same.

In vivo pharmacology

Callosal silencing. We silenced the contralateral representation of both forelimb and hindlimb representations guided by IOI and by placing a borosilicate pipette

(0.7–1.2 MΩ resistance) in layer 2/3 to inject the GABA$_A$ agonist muscimol (0.9 μL of 10 mM muscimol solution in saline) in between the IOI representations of the two limbs. The recording pipette inserted in the stroked hemisphere was not moved during and after the muscimol injection.

GABA$_B$ blockade. We blocked GABA$_B$ receptors by topical application of CGP52432 on recording site (hS1) as in (Palmer *et al.* 2012), at concentrations known not to cause epileptiform activity (1 μM in physiological solution) (Iurilli *et al.* 2012). We made sure that the craniotomy was covered by the drug solution for 40 min before starting the recordings.

Anatomy

In all animals tested subacutely (2 days) after stroking fS1, the forelimb-IOI signal disappeared (Fig. 2*C*). In this animal group, we checked that the anatomical lateral extent of the stroke was matching the IOI representation of the forelimb before stroke, as well as that the lesion reached the white matter (Fig. 2*B*). Accordingly, mice were deeply anaesthetized by means of I.P. urethane overdose. Next, after confirming the complete absence of any responses to tail/toe pinches and corneal reflexes, animals were transcardially perfused with 50 mL of phosphate buffer 0.1 M, followed by 100 ml of 4% paraformaldehyde (PFA) in 0.1 M phosphate buffer. Brains were post fixed in PFA overnight and afterwards 60 μm thick coronal sections were cut with a sliding microtome (SM2010 R; Leica Biosystems, Nußloch, Germany). Sections were then stained for the neuronal nuclear marker (NeuN). Briefly, sections were incubated in PBS-based blocking solution containing 0.3% Triton and 5% normal goat serum for 2 h on room temperature. Afterwards, the sections were incubated with mouse anti-NeuN (cat. no. ab190195; 1:200; Abcam), 0.2% Triton and 5% normal goat serum at 4°C overnight. Slices were then washed with PBS, mounted with Vectashield and analysed under a fluorescence microscope (Zeiss Axio; Carl Zeiss, Carl Zeiss, Oberkochen, Germany) To analyse lesion size and depth, we used a 5× (Zeiss N-Achroplan, NA 0.15). As shown in Fig. 2*B*, in all tested cases ($n = 5$), both the IOI signal for fS1 and the stroke size covered a cortical surface area having a diameter of ~600 μm and reached the white matter, in line with the results of a previous study (Brown *et al.* 2009).

Statistical analysis

Prism, version 6.0. (GraphPad Software Inc., San Diego, CA, USA) was used. Normality was checked with the D'Agostino & Pearson omnibus test. Normally distributed data were compared using one-way ANOVA. Non-normally distributed data were compared using the Kruskal–Wallis test and, in the case of no multiple

comparison, the Mann–Whitney rank test was used. For comparison of paired data, the Wilcoxon paired test was used. Data are presented as the mean ± SD when data were normally distributed and as medians when the data were not normally distributed. In box plots, the line inside the box is the median, whereas the upper and lower segment of the box represent the 75th and 25th percentile, respectively, and the outer lines represent the whole data range.

Results

Subthreshold-only forelimb inputs in the hindlimb representation of S1 in control mice

In most sensory cortices, the receptive fields assessed by synaptic inputs (subthreshold receptive field) are larger compared to those obtained with spike output measurements (suprathreshold receptive field) (Brecht *et al.* 2003; Medini, 2011). This was true also in the limb representations of S1. We performed *in vivo* whole-cell recordings from layer 2/3 pyramids in hS1 as identified by IOI (see Methods), in normal mice to begin with. As shown in the example of Fig. 1*A*, stimulations of both hind- and fore-limbs gave rise to clearly detectable postsynaptic potentials (PSPs) in hS1 in control mice, although the synaptic responses were significantly smaller upon forelimb stimulation (median: 11.2 *vs.* 4.9 mV, $N = 13$ animals, $n = 25$ cells; Wilcoxon paired test, $P < 0.0001$) (Fig. 1*B*, top). All recorded neurons were receiving synaptic inputs from both the forelimb and the hindlimb, whereas only a minority generated a significant AP response to forelimb stimulation (see example of peristimulus time histogram in Fig. 1*A*, bottom; at the population level, 18 out of 25 neurons gave a significant response to hindlimb stimulation, whereas only three responded to the forelimb stimulation). The quantitative analysis of AP responses was restricted to those cells where there was a significant spike response to at least one limb (see Methods). AP responses to hindlimb stimulation in hS1 were significantly larger compared to those obtained after forelimb stimulation (median: 0.21 and 0.10 spikes s^{-1}) (see example in Fig. 1*A*, bottom peristimulus time histograms, as well as the population values in Fig. 1*B*, bottom). Thus, our data indicate that forelimb-driven synaptic inputs reach all neurons also in hS1, although this synaptic input was able to drive neurons to fire APs only in a minority of cells. This sharpening of receptive fields at suprathreshold level is consistent with the rectifying, non-linear action of the AP threshold (Lu *et al.* 2012).

To express this difference quantitatively, we compared a 'limb preference index' for PSP and AP responses for each recorded neuron. The index is computed as $(H - F)/(H + F)$, where H and F are the peak responses upon independent stimulation of the hindlimb and

forelimb, respectively. Such an index varies from −1 to +1 for neurons responding only to the forelimb or to the hindlimb, respectively, and is 0 for neurons that gave equal responses to stimulation of the two limbs. As expected, in hS1, all neurons had index values higher than 0 or equal to 1 (in the case of AP responses), indicating the dominance of hindlimb responses. A paired statistical analysis showed that responses were more skewed in favour of the hindlimb when APs were compared (Fig. 1*C*, medians of limb preference indexes are 0.38 for PSPs *vs.* 1 for APs, Wilcoxon paired test, $P < 0.0001$).

Recovery from stroke occurs at subthreshold (synaptic input) level

We used IOI to phototrombotically lesion fS1 (Fig. 2*A*) because this method generates reproducible focal lesions (Maxwell & Dyck, 2005). Histological analysis showed that the stroked area size matched the size of the forelimb area as defined by IOI (600–700 μm in diameter) and that lesions were reaching the white matter (Fig. 2*B*). To control for the focality of the lesion, we analysed the IOI maps in the subacute phase, 2 days after stroke (Fig. 2*C*). The functional mapping showed that hS1 was spared by the stroke, whereas the representation of the forelimb was no longer detectable (see Methods).

Because hS1 and fS1 are neighbouring areas, we took the changes of synaptic responses to forelimb stimulation in hS1 over time as a measure of the plasticity occurring in the stroke periphery. We compared the subacute effects of the stroke (2 days) with those occurring after a longer recovery (2 weeks) with IOI-targeted *in vivo* whole-cell recordings in hS1 after stroke in fS1. The amplitudes of the PSPs induced by hindlimb stimulation in hS1 did not change neither after 2 days, nor by 2 weeks post-stroke (controls: 11.2 ± 5.8 mV *vs.* 2 days post-stroke: 12.4 ± 4.9 mV, $N = 9$ animals, $n = 20$ cells *vs.* 2 weeks post-stroke recovery group: 10.5 ± 4.8 mV, $N = 11$ animals, $n = 28$ cells; $F_{2,70} = 0.77$, $P = 0.47$, one-way ANOVA test; $r^2 = 0.02$) (Fig. 3*A*, top), confirming the spatial selectivity of the stroke at functional level. The same was true for hindlimb-evoked AP responses (controls: 0.21 spikes s^{-1} *vs.* 2 days post-stroke 0.26 spikes s^{-1}, $N = 9$ animals, $n = 9$ responsive cells *vs.* 2 weeks post-stroke 0.17 spikes s^{-1}, $N = 11$ animals, $n = 16$ responsive cells; Kruskal–Wallis test, $P = 0.94$) (Fig. 3*A*, bottom;). On other hand, forelimb-evoked responses in the same cells decreased dramatically after 2 days from stroke, whereas a significant recovery was observed thereafter (2 weeks after stroke). PSP responses to forelimb in hS1 dropped from 4.9 mV to 2.4 mV after 2 days and recovered to 3.6 mV after 2 weeks (median values are given; Kruskal–Wallis test followed by *post hoc* tests, $P = 0.001$) (Fig. 3*B*, top). The fact that forelimb responses in hS1 dropped right after stroke of fS1 indicates that they originate from fS1-to-hS1

intracortical connections that are destroyed as a consequence of stroke. After 2 weeks from stroke, responses recovered also at suprathreshold level: no neuron was responsive with detectable AP responses 2 days after stroke, whereas we observed that, after 2 weeks, a minority of cells gave rise to detectable AP responses, to a similar extent observed in controls (four out of 28 neurons in 2 weeks recovered animals compared to three out of 25 neurons in controls). Also, the absolute values of these responses attained statistically similar amplitudes, with identical medians (0.1 spikes s^{-1}; Mann–Whitney rank test, $P = 0.74$).

Lack of changes in intrinsic excitability and longer latencies of recovered synaptic responses

Excitability of neurons in the periinfarct area has been reported to change after stroke. For example, down-regulation of phasic inhibition (Schiene *et al.* 1996; Imbrosci *et al.* 2013) accompanied by upregulation of NMDA receptors (Lee *et al.* 1999) has been reported and, simultaneously, an increase in tonic inhibition with behavioural relevance for recovery has been documented (Clarkson *et al.* 2010). However, the net effect of such changes in the intact network *in vivo* remains elusive.

Surprisingly, we failed to observe significant changes in the main parameters that measure intrinsic excitability of layer 2/3 pyramidal neurons, such as V_m values (mean: -67.1 ± 12.8 mV in controls, -68.0 ± 13.5 mV 2 days after stroke, -66.0 ± 15.7 mV 2 weeks after stroke; $F_{2,70} = 0.1206$, $P = 0.89$, one-way ANOVA test; $r^2 = 0.003$) (Fig. 4*A*) and spontaneous AP rates (median: 0.003 Hz in controls, 0.005 Hz 2 days after stroke, 0.020 Hz 2 weeks after stroke; Kruskal–Wallis test, $P = 0.76$) (Fig. 4*B*). Another important parameter describing the intrinsic AP generating mechanism is the AP threshold measured as the V_m value at the time point of V_m maximal acceleration right before AP peak (Wilent & Contreras, 2005). Also in this case, we did not find significant differences among experimental groups, albeit a non-significant trend for increased AP threshold values (suggesting hypoexcitability) was observed (mean: -41.3 ± 4.1 mV in controls, -37.0 ± 6.1 mV in 2 days after stroke, -37.5 ± 5.8 mV in 2 weeks after stroke; $F_{2,34} = 2.49$, $P = 0.1$, one-way ANOVA test; $r^2 = 0.13$) (Fig. 4*C*).

Comparing the temporal kinetics of the recovered synaptic responses with those obtained from controls can give hints on their possible synaptic origin. Accordingly, we compared peak latencies of the synaptic responses upon forelimb stimulation in the controls and 2 weeks
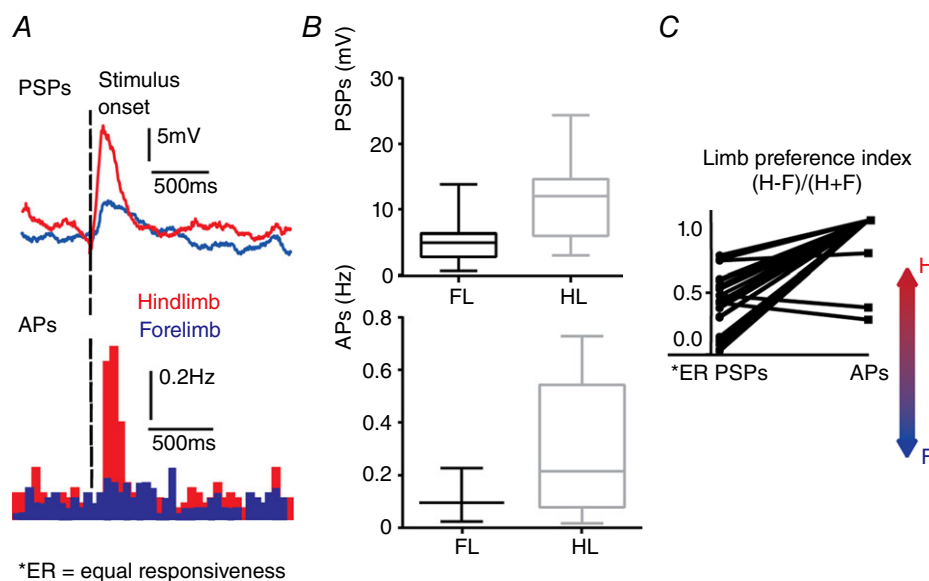

Figure 1. Hindlimb S1 neurons receive subthreshold-only forelimb inputs in control mice
A, top: example of averaged PSPs driven by hindlimb (red) and by forelimb (blue) stimulation, recorded from a layer 2/3 pyramidal neuron in hS1. Sweeps were averaged over 30 presentations. Bottom: peristimulus time histograms for AP counts of the same neuron (bin 50 ms). Note that forelimb stimulation evoked a subthreshold depolarization that doesn't drive the neuron to fire APs. *B*, top: PSP responses upon forelimb (FL) and hindlimb (HL) stimulation; bottom: significant AP responses upon forelimb (FL) and hindlimb (HL) stimulation. *C*, plot showing the relative preference index for the hindlimb and forelimb for each hS1 neuron, calculated for PSP and AP responses, separately. The index was calculated as $(H - F)/(H + F)$, where H and F are the peak responses to hindlimb and forelimb stimulation. The limb preference of AP responses was more skewed towards the hindlimb compared to PSPs (Wilcoxon paired test, $P < 0.0001$). [Colour figure can be viewed at wileyonlinelibrary.com]
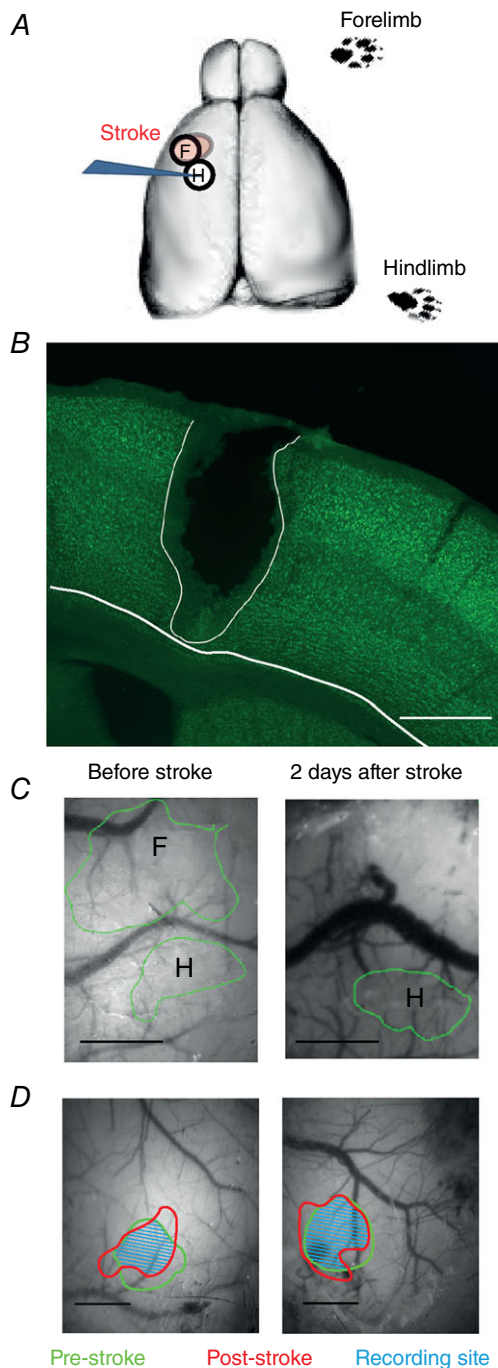
Figure 2. Anatomical and functional controls of the focal stroke model

A, sketch of the experimental stroke protocol, showing an IOI-guided phototrombotic stroke in the forelimb representation (*F*) in S1. Note that all recordings were performed in the neighboring hindlimb representation (*H*). The contralateral limbs were stimulated. *B*, anatomical control of the size of the phototrombotic stroke. The lesioned area matched the size of the forelimb area as defined by IOI (600–700 μm in diameter) and the lesion was reaching the white matter. Section thickness = 60 μm. Scale bar = 500 μm. *C*, IOI was used for cortical mapping of fS1 and hS1 in controls, as well as to position the fibre to induce focal stroke in fS1 (left image). IOI was also used to confirm the spatial selectivity of the lesion after 2 days (right image). Scale bars = 500 μm. *D*, comparison of the hindlimb cortical representations as defined by IOI right before the stroke and at the time of recording. All the recordings were perform within the area of overlap between the pre-stroke and post-stroke hindlimb representation. The IOI spots are drawn on the pre-stroked 'green' vasculature image. Scale bars = 500 μm. [Colour figure can be viewed at wileyonlinelibrary.com]

stroked mice. Recovered synaptic responses had longer peak latencies compared to controls (median: 143 *vs.* 120 ms, Mann–Whitney rank test, $P = 0.02$) (Fig. 4*D*), suggesting the possibility that recovery might be due to plasticity of long-range connections projecting to hS1.

Similar assessment of stroke-induced plasticity with whole-cell and local field potential recordings

Extracellular LFPs integrate synaptic responses within a radius of $\sim$250 μm (Katzner *et al.* 2009). To confirm whether LFPs can be used to assess stroke-induced synaptic plasticity in the stroke periphery, we analysed the changes in LFPs recorded from layer 2/3 in hS1 in response to different limb stimulation before and after stroke (2 days and 2 weeks, as we did for our *in vivo* whole-cell recording series). Stroke-induced plasticity can be quantified by the change in the relative strength of hindlimb- and forelimb-responses, as quantified by the *H-F* index. Thus, we compared the distributions of the *H-F* indexes for *in vivo* whole-cell recordings and for LFP recordings within each experimental groups ($N = 7$ for controls, $N = 6$ for 2 days after stroke, $N = 9$ for 2 weeks after stroke). The distributions of *H-F* indexes obtained with LFPs and *in vivo* whole-cell recordings, respectively, were statistically comparable within each experimental group (median: for PSPs and LFPs are reported; left: 0.38 *vs.* 0.29 for controls; middle: 0.64 *vs.* 0.78 for 2 days after stroke; right: 0.44 *vs.* 0.29 for 2 weeks after stroke; Mann–Whitney rank tests, $P = 0.73$, 0.39 and 0.10, respectively) (Fig. 5). Thus, *in vivo* whole-cell recordings and LFP recordings provide a comparable assessment of stroke-induced plasticity in layer 2/3 in our experimental model.

GABA$_B$-dependent interhemispheric inhibition (IHI) in controls

Increased activation of the contralesional hemisphere as a consequence of stroke has been observed previously, although its extent depends on many factors, such as timing, size of the lesion and the technical approach employed (Caleo, 2015). Most importantly, the functional role of callosal connectivity in the process of recovery of function remains uncertain because controversial results have been obtained by different groups (Di Pino *et al.* 2014). Having shown that the recovered synaptic responses

had longer than normal latencies, we wanted to examine how silencing of contralateral S1 influenced the recovered sensory responses in the stroke periphery in our lesion model.

We started with control mice by recording LFP responses of layer 2/3 hS1 to independent stimulation forelimb and hindlimb, before and after acute pharmacological silencing of both limb representation in contralateral S1 (Fig. 6A). In the control group, silencing contralateral S1 caused a dramatic increase in sensory responses to separate stimulation of both limbs (median LFP peak responses for hindlimb: 452 μV *vs.* 2918 μV before and after contralateral S1 silencing, respectively; for forelimb: 287 μV before *vs.* 1156 μV after silencing; $N = 7$ animals; Wilcoxon paired tests, $P = 0.01$) (Fig. 6B, representative examples on the left, grand averages in the middle, and a plot showing the paired statistics on the right; hindlimb and forelimb responses are shown on the top and bottom rows, respectively). These data indicate that, in controls,
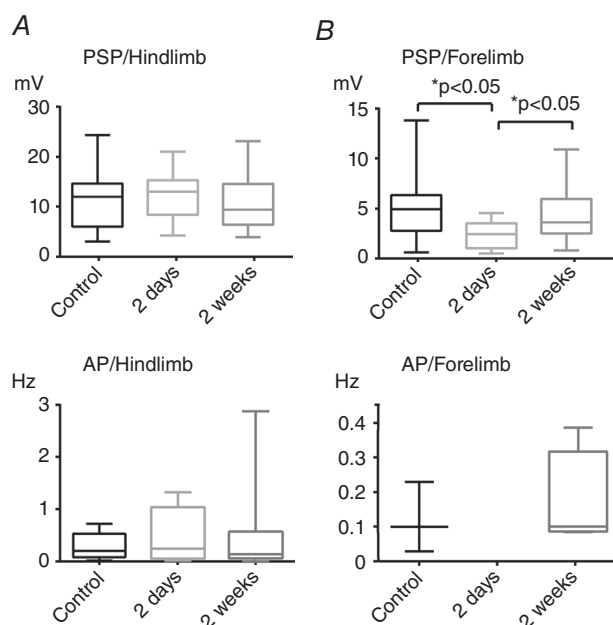
one hemisphere powerfully inhibits contralateral S1, in line with previous studies (Ferbert *et al.* 1992; Gerloff *et al.* 1998; Di Lazzaro *et al.* 1999; Grefkes *et al.* 2008).

The time windows for our analysis was in the interval 0–300 ms after stimulus onset (see Methods). Because the FP responses were often biphasic, with a first peak occurring before 100 ms and a second one occurring between 100 and 300 ms (see example with dashed line in the grand average shown in Fig. 6B), we repeated the analysis to control whether the IHI was differentially occurring in these two time windows. Our results showed that this was not the case. Indeed, forelimb responses increased upon muscimol blockade from a median value of 255 μV to 1156 μV (Wilcoxon paired test, $P = 0.01$) when the peak was searched in the 0–100 ms time window and from 286 μV to 967 μV (Wilcoxon paired test, $P = 0.01$ time window 100–300 ms). The same was true for hindlimb responses (0–100 ms; median: 452 μV *vs.* 2918 μV, Wilcoxon paired test $P = 0.01$, 100–300 ms: 660 μV *vs.* 2498 μV, Wilcoxon paired test, $P = 0.03$).

IHI has been proven to be mediated by GABA$_B$ receptors in rat hS1 (Palmer *et al.* 2012). We aimed to control whether the IHI that we documented in mouse S1 is also GABA$_B$-dependent. Accordingly, we topically applied the GABA$_B$ blocker CGP52432 (at a concentration of 1 μM; Iurilli *et al.* 2012; Palmer *et al.* 2012) before starting LFP recordings (Fig. 6C). Under GABA$_B$ blockade, responses did not increase after contralateral silencing. In other words, we failed to observe any sign of IHI (as an example, see the grand averages and paired data plot in Fig. 6D). By contrast, we observed a non-significant trend for response reduction upon contralateral S1 silencing under GABA$_B$ blockade (median: 288 μV *vs.* 99 μV before and after contralateral S1 silencing, respectively; $N = 5$ animals; Wilcoxon paired test, $P = 0.06$). The observed trend for a decreased response amplitude after callosal silencing under GABA$_B$ blockade can be explained by the fact that, under GABA$_B$ blockade, the callosal pathway has a 'pure' excitatory influence on the recording site that is not masked by IHI (see callosal pathway depicted in orange in Fig. 8A). As a result, callosal silencing in these conditions reduces the sensory response measured before silencing because the latter is the summed response of the callosal and of the direct activation by the contralateral limb (depicted in orange and green, respectively in Fig. 8A). Overall, these results indicate that the IHI we documented is GABA$_B$-mediated, in line with the previous report in rat hS1 (Palmer *et al.* 2012).

Figure 3. Recovery of sensory synaptic responses 2 weeks after stroke
A, no effect of stroke on the hindlimb responses in hS1. Top: PSP responses upon hindlimb stimulation in hS1 in controls, 2 days and 2 weeks after stroke were statistically comparable ($F_{2,70} = 0.77$, $P = 0.47$, one-way ANOVA test; $r^2 = 0.02$), confirming the focal nature of the lesion protocol. Bottom: AP responses upon hindlimb stimulation in hS1 in controls, 2 days and 2 weeks after stroke were also statistically comparable (Kruskal–Wallis test, $P = 0.94$). *B*, recovery of sensory responsiveness to forelimb stimulation in hS1. Top: PSP responses upon forelimb stimulation in hS1 in controls, 2 days and 2 weeks after stroke. Note the recovery of spike responses after 2 weeks (Kruskal–Wallis test followed by *post hoc* tests, $P = 0.001$). Bottom: APs upon forelimb stimulation in hS1 in controls, 2 days and 2 weeks after stroke (median: 0.1 spikes s^{-1}; Mann–Whitney rank test $P = 0.74$).

Loss of IHI and facilitation of recovered responses of callosal origin in stroke periphery

The same approach was then used in animals after 2 weeks of recovery from the phototrombotic stroke (Fig. 7A). Unexpectedly, we did not find any evidence of the powerful

IHI normally observed in controls in this case. Responses to stimulation of hindlimb were statistically comparable before and after muscimol silencing of contralateral hemisphere, showing no sign of IHI. Not only we did not observe any sign of response increase but a trend to a decrease actually was observed for hindlimb responses in hS1 that was far from being significant (median value of LFP before 631 μV vs. 246 μV after contralateral silencing; $N = 9$ animals; Wilcoxon paired test, $P = 0.3$) (Fig. 7B, top row). Of relevance, the recovered responses to stimulation of forelimb were instead significantly (two-fold) reduced after inactivation of contralateral S1 (median value of LFP before and after contralateral silencing 471.8 μV vs. 70 μV, respectively; $N = 9$ animals, Wilcoxon paired test, $P = 0.008$) (Fig. 7B, bottom row).

In summary, our data indicate a dramatic loss of IHI of synaptic sensory responses on the stroke periphery compared to controls, accompanied by a pathway-specific facilitation of recovered responses of callosal origin.
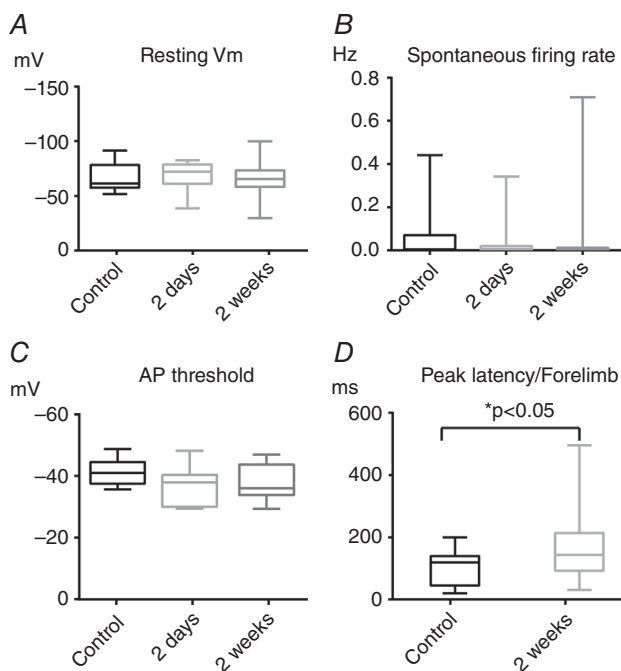

Figure 4. Lack of changes in intrinsic neuronal excitability in stroke periphery and longer latencies of recovered synaptic responses

A, resting V_m values showed no significant difference among groups (controls, 2 days and 2 weeks after stroke; $F_{2,70} = 0.1206$, $P = 0.89$, one-way ANOVA test; $r^2 = 0.003$). B, median values of spontaneous firing rates were statistically comparable among groups (Kruskal–Wallis test, $P = 0.76$). C, AP thresholds values did not show statistically difference among groups ($F_{2,34} = 2.49$, $P = 0.1$, one-way ANOVA test; $r^2 = 0.13$). D, comparison of the peak latencies of the synaptic responses 2 weeks after stroke upon forelimb stimulation with those of control animals. Note the longer latencies of the recovered synaptic responses (Mann–Whitney test, $P = 0.02$).

Discussion

We investigated the sub- and suprathreshold effects of stroke-driven plasticity in the excitatory network of a functionally identified region in mouse S1 using a focal stroke model. Recovery from stroke in the lesion periphery occurred primarily at subthreshold (synaptic input) level, without gross changes in neuronal intrinsic excitability. We found that the source of synaptic recovery was the homotopic region of the contralateral hemisphere. In particular, the usually strong GABA$_B$-mediated IHI present in controls was absent in the stroke periphery and was replaced instead by a pathway-specific facilitation of the recovered sensory response of callosal origin.

Plasticity of local microcircuits after stroke: sub- vs. suprathreshold effects

Around brain lesions, hypoexcitability is followed by hyperexcitability and then by sensory input remapping (Carmichael, 2012). Changes in both excitatory and inhibitory transmissions occur. Schiene et al. (1996) and Imbrosci et al. (2013) reported decreased phasic inhibition coupled with hyperexcitability, whereas (Clarkson et al. 2010) showed an increase of tonic inhibition that was behaviourally relevant. Furthermore, excitatory NMDA currents increase in stroke periphery (Huemmeke et al. 2004) and this is accompanied by a time-dependent AMPA current modulation (Clarkson et al. 2011). However, the net effect on local microcircuits in vivo remains unclear. Our data suggest that such changes might balance each other to some extent. Indeed, V_m, spontaneous AP rates and AP threshold were normal in lesion periphery. Because in vivo whole-cell recordings are taken mostly from somatas (Margrie et al. 2002), we cannot exclude changes in dendritic excitability (e.g. as a result of modifications of ion channel composition). Moreover, because we intracellularly recorded layer 2/3 pyramids, we cannot exclude changes in the intrinsic excitability of deeper (e.g layer 5) neurons in that callosal influences are layer-specific (Palmer et al. 2013). A major change of the excitability of GABAergic cells appears improbable because V_m, spontaneous AP rates and AP threshold are sensitive to modifications of GABAergic transmission (Caillard, 2011). Taken together, our data indicate that post-stroke recovery of sensory responsiveness is largely a result of changes in the synaptic inputs received by neurons in the stroke periphery rather than changes in their AP generating mechanism.

Plasticity of interarea connections after stroke: effects of callosal inputs on stroke periphery

hS1 neurons display subthreshold-only responses also to forelimb stimulation in controls. Such responses presumably originate from excitatory fS1-to-hS1

connections because they disappear subacutely after fS1 lesioning. Moreover, we show that contralateral S1 inhibits sensory responses in controls. Thus, our data suggest that in hS1 interhemispheric, inhibitory connections, antagonize horizontal, excitatory connections from fS1 (Fig. 8*A*). This antagonism is in line with callosal fibres sharpening tactile fields in rat S1 (Palmer *et al.* 2012).

In the complex and still controversial literature on the role of callosum on stroke recovery there is, at least to some degree, consensus that: (i) contralesional activation is size-dependent, being larger for larger lesions (Grefkes *et al.* 2008; Di Pino *et al.* 2014); (ii) this activation appears to be beneficial for larger lesions and detrimental for smaller ones (Biernaskie *et al.* 2005); and (iii) in case of small lesions, an initial contralesional activation is followed by re-activation of perilesional areas, with this re-activation correlating with functional recovery (Dijkhuizen *et al.* 2001).

However, clinical studies show that the role of the contralateral activation in stroke recovery remains controversial. Indeed, transcranial magnetic stimulation (TMS) inhibiting the contralesional hemisphere interfered with neurological recovery (Dancause *et al.* 2015), whereas other studies showed no benefit (Talelli *et al.* 2007, 2012) or even a facilitatory action (Butefisch *et al.* 2003; Song *et al.* 2005; Bradnam *et al.* 2012).

Importantly, attempts to promote stroke recovery by inhibiting the contralesional hemisphere rest on the so called 'interhemispheric competition model', which is based on the idea that inhibiting the healthy hemisphere will facilitate recovery by reducing IHI on the stroked hemisphere (Silasi & Murphy, 2014; Caleo, 2015). Clinical data already showed the necessity of revising such a model (Di Pino *et al.* 2014).

In that respect, our data show that the assumption that IHI persists in the stroke periphery needs to be revisited. Indeed, we show that, in a reproducible model of focal stroke, the normal interhemispheric suppression of sensory responsiveness observed in controls is simply not detectable in the stroke periphery. Instead, we found a switch of the action of callosal input from inhibitory to facilitatory because contralateral S1 silencing selectively suppresses the recovered (forelimb) responses, without affecting the hindlimb responses, whereas, in controls, the same manipulation caused dramatic increases of limb responses.

Second, our data, taken together with the existing literature, indicate a postsynaptic origin of this switch within the network of the stroke periphery. Indeed, forelimb responses increase in the contralesional hemisphere in a similar mouse model of S1 stroke (Takatsuru *et al.* 2009) and increased contralesional activation and synaptic remodelling after stroke in S1 was also shown by (Biernaskie & Corbett, 2001; Reinecke *et al.* 2003). Thus, if IHI from the healthy side would have still been present, we should have observed an even larger percentage increase of responsiveness in stroke periphery after contralateral silencing as a result of the hyperactivation of the contralesional hemisphere. The fact that, instead, we failed to see any increase of responsiveness after contralateral silencing in stroked animals argues in favour of the idea that the synaptic change(s) responsible for lack of IHI must have occurred locally in the microcircuits of the stroke periphery. Furthermore, the fact that contralateral silencing caused a response reduction both in controls under GABA$_B$ blockade and on stroke-recovered responses is in line with the view that GABA$_B$-dependent IHI is lost in the stroke periphery (Fig. 8).
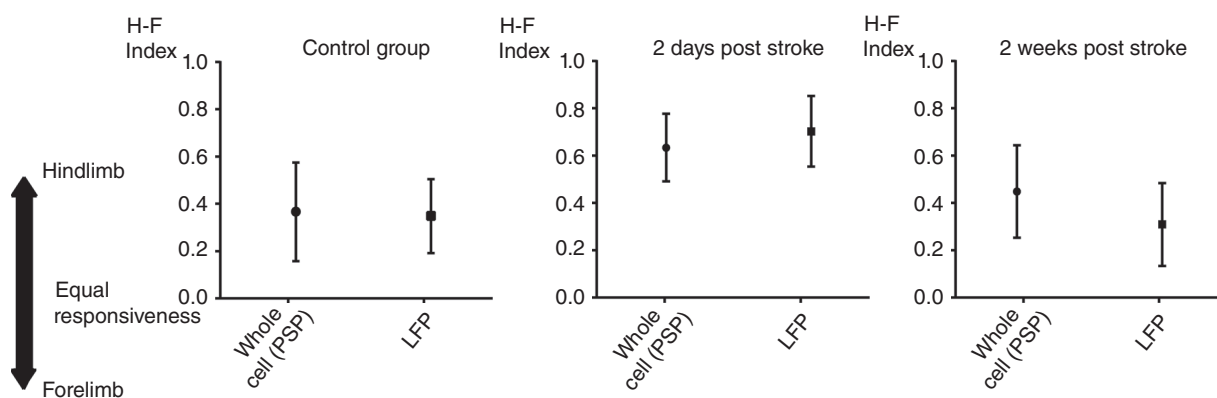

Figure 5. Similar assessment of stroke-induced synaptic plasticity with whole-cell recordings and local field potentials
The distributions of the *H-F* indexes, which express the relative strength of the synaptic inputs driven stimulation of the two limbs, were comparable within each experimental group, when calculated after *in vivo* whole-cell recordings and LFPs (controls: left; 2 days after stroke: middle; 2 weeks after stroke: right; Mann–Whitney rank tests, *P* = 0.73, 0.39 and 0.10, respectively). Data are the mean ± SD.
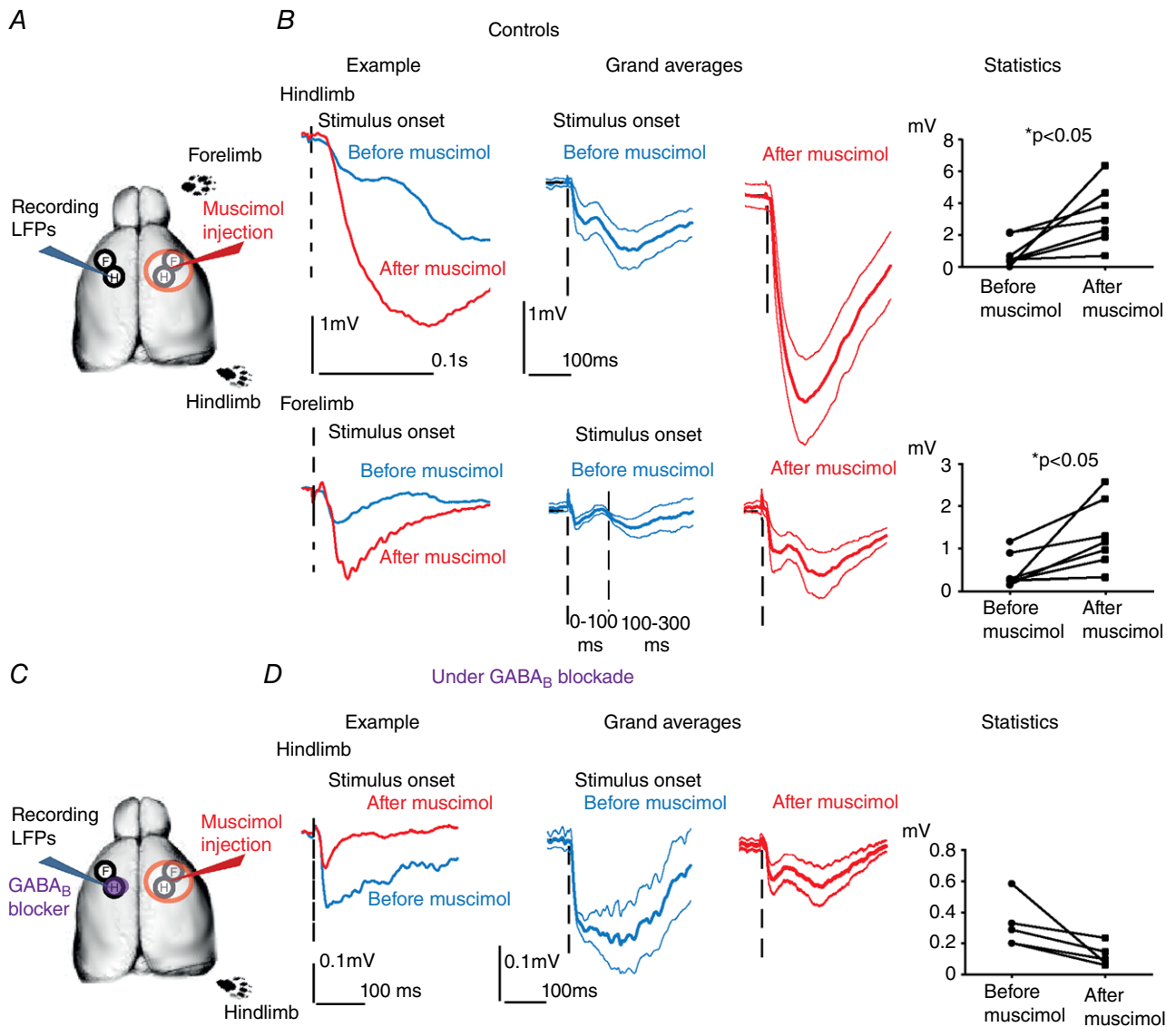
Figure 6. GABA$_B$-dependent interhemispheric inhibition in controls

A, experimental sketch for LFPs from hS1 before and after acute silencing of contralateral S1 with muscimol in controls. *B*, interhemispheric inhibition in controls. Left: examples of LFP responses to separate stimulation of the hindlimb (top) and of the forelimb (bottom) before (in blue) and after (in red) silencing contralateral S1. Note the dramatic increase of sensory responses. Middle: comparison of the grand averages of the LFP responses to hindlimb (top) and forelimb (bottom) before and after contralater S1 silencing (blue and red, respectively). Mean ± SEM values are shown by the thick and thinner lines, respectively. Sensory responses significantly increase after inactivation of contralateral hemisphere. Right: paired statistical comparisons of the amplitudes of the sensory responses to separate hindlimb (top) and forelimb (bottom) stimulation before and after contralateral S1 silencing show a significant increase (Wilcoxon paired tests, *P* = 0.01). *C*, experimental sketch for LFPs from hS1 before and after acute silencing of contralateral S1 with muscimol under GABA$_B$ blockade in the recording site, done in controls. *D*, interhemispheric inhibition was not observed under GABA$_B$ blockade in controls. Left: example of LFP responses to hindlimb stimulation in hS1 before (in blue) and after (in red) silencing contralateral S1. Note that there is non-significant trend for response reduction upon contralateral S1 silencing under GABA$_B$ blockade. Middle: comparison of the grand averages of the LFP responses to hindlimb before and after contralater S1 silencing (blue and red, respectively). Mean ± SEM values are shown by the thick and thinner lines, respectively. Sensory responses non-significantly decrease after inactivation of contralateral hemisphere. Right: paired statistical comparisons of the amplitudes of the sensory responses to hindlimb stimulation before and after contralateral S1 silencing show non-significant decrease under GABA$_B$ blockade (Wilcoxon paired test, *P* = 0.06). [Colour figure can be viewed at wileyonlinelibrary.com]

In our stroke model, contralateral S1 silencing had no effect on hindlimb but suppressed recovered forelimb-responses in stroke periphery, suggesting the co-existence of: (i) a generalized reduction of IHI and (ii) a selective facilitation of recovered responses of callosal origin. A plausible mechanism underlying the latter observation could be a higher activation of the contralesional fS1 (compared to the contralesional hS1), as a result of interhemispheric innervation and the accompanying inhibition presumably being denser for somatotopically corresponding regions in mouse S1 (Wise & Jones, 1976; Zhou *et al.* 2013).

Possible synaptic and molecular mechanisms of interhemispheric plasticity

IHI is present both in human and rodents S1. Callosal connections activate layer 1 interneurons that in turn inhibit layer 5 neurons via $GABA_B$ receptors (Palmer *et al.* 2012). Contralateral silencing did not increase sensory responses in controls under $GABA_B$ blockade,

indicating that the IHI we have studied in the present study is $GAABA_B$-mediated, presumably relying on the same cellular mechanism described by Palmer *et al.* (2012). Interestingly, $GABA_B$ receptors play also a role in IHI in humans (Irlbacher *et al.* 2007). What could be the cellular mediator of IHI and how could this subcircuit be affected by stroke? One candidate are neurogliaform cells, which can generate long-lasting inhibition in many neighbouring pyramids (Rudy *et al.* 2011).

One economical explanation of our results could be that layer 1 interneurons in hS1 mediating IHI are more sensitive to ischaemia compared to pyramids. However, this does not appear to plausible because global ischaemia not only does not cause such a loss, but instead triggers neurogenesis of GABAergic cells selectively in layer 1 (Ohira *et al.* 2010).

An alternative explanation could instead be pruning or retraction of callosal synapses from the layer 1 interneurons responsible for IHI, possibly accompanied by a potentiation of the direct effect of glutameric callosal
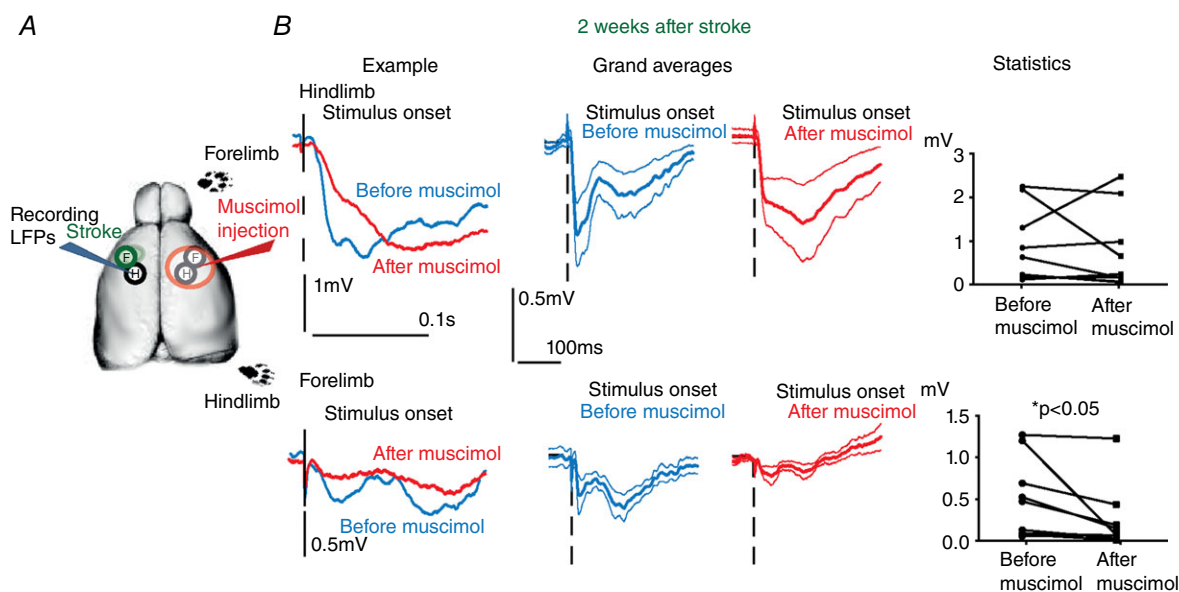

Figure 7. Loss of interhemispheric inhibition and selective facilitation of recovered responses of callosal origin in the stroke periphery

A, experimental sketch for LFPs from hS1 before and after acute silencing of contralateral (contralesional) S1 with muscimol in the animals that displayed full recovery (2 weeks after stroke). *B*, loss of interhemispheric inhibition after recovery from stroke. Left: example of LFP responses to separate stimulation of the hindlimb (top) and of the forelimb (bottom) before (in blue) and after (in red) silencing contralateral S1. Note that the response to hindlimb did not show the dramatic increase of sensory responses observed in controls, whereas a reduction of the response to forelimb stimulation was observed. Middle: comparison of the grand averages of the LFP responses to hindlimb (top) and forelimb (bottom) before and after contralateral S1 silencing (blue and red, respectively). Mean ± SEM values are given. In this case, sensory responses to hindlimb stimulation were not significantly affected by contralateral S1 silencing (top), whereas the recovered forelimb responses were almost suppressed by the same manipulation. Right: paired statistical comparison of the amplitudes of the sensory responses to separate hindlimb (top) and forelimb (bottom) before and after contralateral S1 silencing. Note the lack of effect of contralateral S1 silencing for hindlimb responses after callosal silencing (top: Wilcoxon paired test, $P = 0.3$), whereas forelimb responses showed a significant decrease after the very same manipulation (Wilcoxon paired test, $P = 0.01$). [Colour figure can be viewed at wileyonlinelibrary.com]

fibres onto local pyramids (see the model proposed in Fig. 8*B*).

We observe callosal-dependent recovery of responses 2 weeks but not 2 days after stroke, suggesting that slow, structural rearrangements might have occurred. This is plausible as two-photon imaging showed dendritic remodelling after stroke, with increased spine formation in stroke periphery peaking when functional plasticity is also maximal (Brown *et al.* 2007, 2010). Such processes are accompanied by upregulation of axonal growth markers such as GAP-43 (Caleo, 2015) and CAP 23 (Caleo, 2015), as well as growth inhibiting factors such as ephrin-A5 (Overman *et al.* 2012) and chondroitin sulphate proteoglycans (Soleman *et al.* 2012; Quattromani *et al.* 2018), which are known to play a role in functional recovery.

Behavioural relevance

The role of callosal input in recovery after human stroke remains controversial and a matter of debate, as effectively summarized by (Buetefisch, 2015): 'Meta-analyses on the effectiveness of repetitive transcranial magnetic stimulation or transcranial direct current stimulation in stroke rehabilitation therapy do not agree on the available evidence to either support or reject it'.

Our results indicate that IHI is not detectable in the stroke periphery of mouse S1 at a time point where recovery of responsiveness was complete. It is not straightforward to compare the result of our direct pharmacological inactivation with the clinical results using TMS because the cellular mechanisms and the net effects of TMS protocols on microcircuits remain largely unknown. Even a simple TMS pulse recruits the very same dendritic inhibitory mechanisms involved in IHI (Murphy *et al.* 2016), implying that even a single TMS pulse is certainly not purely excitatory. Species-specific differences, as well as the possible effect of lesion size on interhemispheric interactions after stroke, could also explain some discrepancies with the clinical literature.

Our view on the relevance of our results for functional recovery after stroke is that the loss of IHI in the stroke periphery could play a permissive role for the plasticity of those excitatory connections (that we have shown to be also of callosal origin) underlying recovery of neuronal responsiveness. Indeed, a reduction of inhibitory neurotransmission facilitates experience-dependent plasticity *in vivo* because the strength of inhibitory connections is one of the major determinants for the opening and closure of the critical period for ocular dominance plasticity in the primary visual cortex, a classical paradigm of experience-dependent plasticity (Hensch *et al.* 1998; Huang *et al.* 1999; Harauzov *et al.* 2010). Inhibition is indeed a determinant of the temporal integration properties of synapses (Pouille & Scanziani, 2001), which is the core mechanism underlying input-specific plasticity. More strictly related to our work, diminution of inhibitory neurotransmission in the stroke periphery (Mittmann *et al.* 1994) is indeed accompanied by a facilitation of classical forms of synaptic plasticity, such as long-term potentiation (Mittmann & Eysel, 2001).

There are behavioural observations conducted out in preclinical models very close to ours (focal strokes in rodent S1) that are in line with our observations. It was
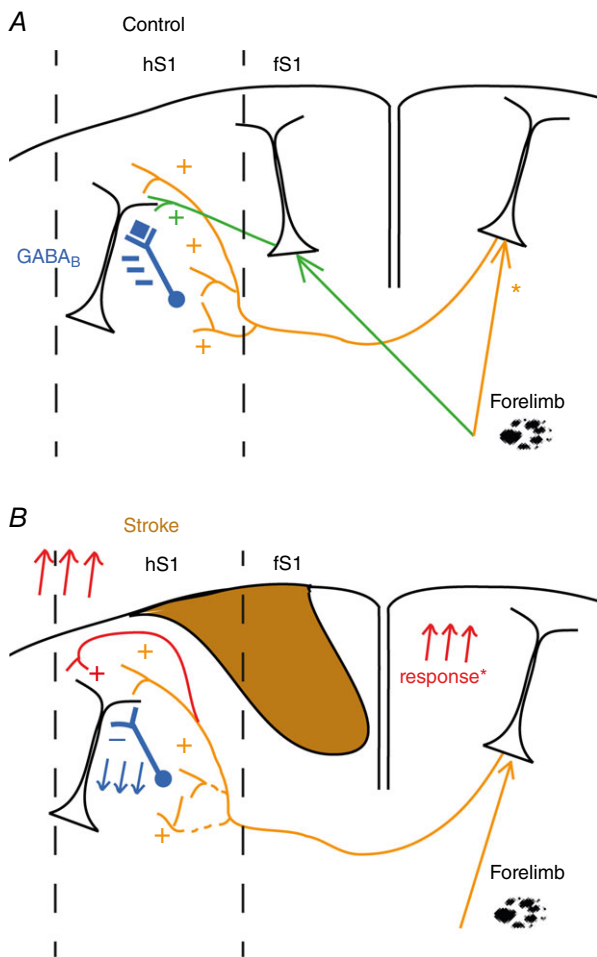

Figure 8. Proposed model of the synaptic changes occurring in callosal connectivity in the periphery of a focal stroke
A, normal condition: callosal inputs (orange pathway) inhibits sensory responses mediated by the direct activation of the contralateral limb (green pathway) via activation of locally residing interneurons that act via GABA_B (blue). *Under normal conditions limb tactile stimulation activates the ipsilateral cortex (e.g. (Takatsuru *et al.* 2009); Kokinovic and Medini, unpublished observation). *B*, after a focal stroke, recovery of forelimb responses cannot occur via horizontal connections from the stroked area. Instead, recovery happens via the combined effect of reduced strength of IHI (blue) and by potentiation of the direct callosal excitatory input (red). The latter can be accounted for increased strength of the local excitatory synapses present in the stroke periphery and/or by an increased activation of the contralesional cortex (Reinecke *et al.* 2003; Takatsuru *et al.* 2009). [Colour figure can be viewed at wileyonlinelibrary.com]

reported previously that lidocaine contralesional silencing indeed counteracted the behavioural recovery of the affected limb in a way that was dependent on the lesion size (Biernaskie *et al.* 2005). In addition, a significantly decreased function of the recovered forelimb was found after acute lesioning of the previously healthy hemisphere (Shanina *et al.* 2006), after one full week from the initial stroke, and a trend for a decreased function was observable but not significant at later times.

For the sake of completeness, the results of studies where chronic silencing (Mansoori *et al.* 2014) or callosotomy (Jin *et al.* 2011) were performed simultaneously with the stroke induction could also be discussed. However, it is difficult to compare possible behavioural extrapolations of our results with these studies because the effects of acute silencing experiments are testing more directly the actual role of the corpus callosum on the already recovered functional outcome. In addition, such studies also report conclusions that, to a significant extent, are not consistent with each other because chronic silencing is worsening the behavioural outcome, even though callosotomy did not affect the behavioural recovery.

Accordingly, any interpretation of the results of contralesional silencing experiments should take into account possible deficits caused by the acute silencing on the function on the initially unaffected limb. Indeed, the interpretation of the data of tests that measure the relative use of the two forelimbs (such as the glass cylinder test and the foot-fault test) could be affected by this type of ipsilesional deficit. Even when the performance of a motor act performed by a single limb is measured (such as in reaching and grasping tests), the performance of a certain limb during ipsilateral silencing can be affected by postural deficits imposed to the limb contralateral to the acutely silenced hemisphere (a phenomenon clearly present also in controls) (Biernaskie *et al.* 2005). Thus, our results, taken together with other studies that are beginning to clarify the circuits mediating IHI *in vivo*, prompt the need to perform such experiments during selective (e.g. optogenetic) silencing of callosally projecting neurons and circuits (that are now at least partially known) (Palmer *et al.* 2012). The latter is indeed a manipulation that should minimize ipsilesional forelimb deficits on one side as a result of the lower number of neurons affected and also because callosally projecting cells usually do not project subcortically(Molnar & Cheung, 2006). By contrast, if such deficits are anyhow measurable, they should be taken into account in the data interpretation.

Generalized relevance for other cortical areas

Could these findings in S1 be extended to other cortical areas, where the synaptic circuits mediating interhemispheric communication could differ? Indeed, interhemispheric inputs are primarily excitatory in visual areas, as demonstrated by the reduced binocularity of visual cortical neurons after callosal inactivation in both cats (Yinon *et al.* 1992) and rodents (Pietrasanta *et al.* 2012). These data raise the question of whether IHI is area-specific, and additionally, how interhemispheric communication is affected by stroke in non-sensorimotor cortices, such as in visual areas.

References

Biernaskie J, Chernenko G & Corbett D (2004). Efficacy of rehabilitative experience declines with time after focal ischemic brain injury. *J Neurosci* **24**, 1245–1254.

Biernaskie J & Corbett D (2001). Enriched rehabilitative training promotes improved forelimb motor function and enhanced dendritic growth after focal ischemic injury. *J Neurosci* **21**, 5272–5280.

Biernaskie J, Szymanska A, Windle V & Corbett D (2005). Bi-hemispheric contribution to functional motor recovery of the affected forelimb following focal ischemic brain injury in rats. *Eur J Neurosci* **21**, 989–999.

Bradnam LV, Stinear CM, Barber PA & Byblow WD (2012). Contralesional hemisphere control of the proximal paretic upper limb following stroke. *Cereb Cortex* **22**, 2662–2671.

Brecht M, Roth A & Sakmann B (2003). Dynamic receptive fields of reconstructed pyramidal cells in layers 3 and 2 of rat somatosensory barrel cortex. *J Physiol* **553**, 243–265.

Brown CE, Aminoltejari K, Erb H, Winship IR & Murphy TH (2009). In vivo voltage-sensitive dye imaging in adult mice reveals that somatosensory maps lost to stroke are replaced over weeks by new structural and functional circuits with prolonged modes of activation within both the peri-infarct zone and distant sites. *J Neurosci* **29**, 1719–1734.

Brown CE, Boyd JD & Murphy TH (2010). Longitudinal in vivo imaging reveals balanced and branch-specific remodeling of mature cortical pyramidal dendritic arbors after stroke. *J Cereb Blood Flow Metab* **30**, 783–791.

Brown CE, Li P, Boyd JD, Delaney KR & Murphy TH (2007). Extensive turnover of dendritic spines and vascular remodeling in cortical tissues recovering from stroke. *J Neurosci* **27**, 4101–4109.

Butefisch CM, Netz J, Wessling M, Seitz RJ & Homberg V (2003). Remote changes in cortical excitability after stroke. *Brain* **126**, 470–481.

Buetefisch CM (2015). Role of the Contralesional Hemisphere in Post-Stroke Recovery of Upper Extremity Motor Function. *Front Neurol* **6**, 214.

Caillard O (2011). Pre & postsynaptic tuning of action potential timing by spontaneous GABAergic activity. *PLoS ONE* **6**, e22322.

Caleo M (2015). Rehabilitation and plasticity following stroke: insights from rodent models. *Neuroscience* **311**, 180–194.

Carmichael ST (2012). Brain excitability in stroke: the yin and yang of stroke progression. *Arch Neurol* **69**, 161–167.

Clarkson AN, Huang BS, Macisaac SE, Mody I & Carmichael ST (2010). Reducing excessive GABA-mediated tonic inhibition promotes functional recovery after stroke. *Nature* **468**, 305–309.

Clarkson AN, Overman JJ, Zhong S, Mueller R, Lynch G & Carmichael ST (2011). AMPA receptor-induced local brain-derived neurotrophic factor signaling mediates motor recovery after stroke. *J Neurosci* **31**, 3766–3775.

Dancause N, Touvykine B & Mansoori BK (2015). Inhibition of the contralesional hemisphere after stroke: reviewing a few of the building blocks with a focus on animal models. *Prog Brain Res* **218**, 361–387.

Di Lazzaro V, Oliviero A, Profice P, Insola A, Mazzone P, Tonali P & Rothwell JC (1999). Direct demonstration of interhemispheric inhibition of the human motor cortex produced by transcranial magnetic stimulation. *Exp Brain Res* **124**, 520–524.

Di Pino G, Pellegrino G, Assenza G, Capone F, Ferreri F, Formica D, Ranieri F, Tombini M, Ziemann U, Rothwell JC & Di Lazzaro V (2014). Modulation of brain plasticity in stroke: a novel model for neurorehabilitation. *Nat Rev Neurol* **10**, 597–608.

Dijkhuizen RM, Ren J, Mandeville JB, Wu O, Ozdag FM, Moskowitz MA, Rosen BR & Finklestein SP (2001). Functional magnetic resonance imaging of reorganization in rat brain after stroke. *Proc Natl Acad Sci USA* **98**, 12766–12771.

Ferbert A, Priori A, Rothwell JC, Day BL, Colebatch JG & Marsden CD (1992). Interhemispheric inhibition of the human motor cortex. *J Physiol* **453**, 525–546.

Gerloff C, Cohen LG, Floeter MK, Chen R, Corwell B & Hallett M (1998). Inhibitory influence of the ipsilateral motor cortex on responses to stimulation of the human cortex and pyramidal tract. *J Physiol* **510**, 249–259.

Grefkes C, Eickhoff SB, Nowak DA, Dafotakis M & Fink GR (2008). Dynamic intra- and interhemispheric interactions during unilateral and bilateral hand movements assessed with fMRI and DCM. *Neuroimage* **41**, 1382–1394.

Grundy D (2015). Principles and standards for reporting animal experiments in The Journal of Physiology and Experimental Physiology. *J Physiol* **593**, 2547–2549.

Harauzov A, Spolidoro M, DiCristo G, De Pasquale R, Cancedda L, Pizzorusso T, Viegi A, Berardi N & Maffei L (2010). Reducing intracortical inhibition in the adult visual cortex promotes ocular dominance plasticity. *J Neurosci* **30**, 361–371.

Hensch TK, Fagiolini M, Mataga N, Stryker MP, Baekkeskov S & Kash SF (1998). Local GABA circuit control of experience-dependent plasticity in developing visual cortex. *Science* **282**, 1504–1508.

Huang ZJ, Kirkwood A, Pizzorusso T, Porciatti V, Morales B, Bear MF, Maffei L & Tonegawa S (1999). BDNF regulates the maturation of inhibition and the critical period of plasticity in mouse visual cortex. *Cell* **98**, 739–755.

Huemmeke M, Eysel UT & Mittmann T (2004). Lesion-induced enhancement of LTP in rat visual cortex is mediated by NMDA receptors containing the NR2B subunit. *J Physiol* **559**, 875–882.

Imbrosci B, Neubacher U, White R, Eysel UT & Mittmann T (2013). Shift from phasic to tonic GABAergic transmission following laser-lesions in the rat visual cortex. *Pflugers Arch* **465**, 879–893.

Irlbacher K, Brocke J, Mechow JV & Brandt SA (2007). Effects of GABA(A) and GABA(B) agonists on interhemispheric inhibition in man. *Clin Neurophysiol* **118**, 308–316.

Iurilli G, Ghezzi D, Olcese U, Lassi G, Nazzaro C, Tonini R, Tucci V, Benfenati F & Medini P (2012). Sound-driven synaptic inhibition in primary visual cortex. *Neuron* **73**, 814–828.

Iurilli G, Olcese U & Medini P (2013). Preserved excitatory-inhibitory balance of cortical synaptic inputs following deprived eye stimulation after a saturating period of monocular deprivation in rats. *PLoS One* **8**, e82044.

Jin K, Xie L, Sun F, Mao X & Greenberg DA (2011). Corpus callosum and experimental stroke: studies in callosotomized rats and acallosal mice. *Stroke* **42**, 2584–2588.

Katzner S, Nauhaus I, Benucci A, Bonin V, Ringach DL & Carandini M (2009). Local origin of field potentials in visual cortex. *Neuron* **61**, 35–41.

Lee JM, Zipfel GJ & Choi DW (1999). The changing landscape of ischaemic brain injury mechanisms. *Nature* **399**, A7–14.

Lu U, Roach SM, Song D & Berger TW (2012). Nonlinear dynamic modeling of neuron action potential threshold during synaptically driven broadband intracellular activity. *IEEE Trans Biomed Eng* **59**, 706–716.

Mansoori BK, Jean-Charles L, Touvykine B, Liu A, Quessy S & Dancause N (2014). Acute inactivation of the contralesional hemisphere for longer durations improves recovery after cortical injury. *Exp Neurol* **254**, 18–28.

Margrie TW, Brecht M & Sakmann B (2002). In vivo, low-resistance, whole-cell recordings from neurons in the anaesthetized and awake mammalian brain. *Pflugers Arch* **444**, 491–498.

Marshall RS, Perera GM, Lazar RM, Krakauer JW, Constantine RC & DeLaPaz RL (2000). Evolution of cortical activation during recovery from corticospinal tract infarction. *Stroke* **31**, 656–661.

Maxwell KA & Dyck RH (2005). Induction of reproducible focal ischemic lesions in neonatal mice by photothrombosis. *Dev Neurosci* **27**, 121–126.

Medini P (2011). Cell-type-specific sub- and suprathreshold receptive fields of layer 4 and layer 2/3 pyramids in rat primary visual cortex. *Neuroscience* **190**, 112–126.

Mittmann T & Eysel UT (2001). Increased synaptic plasticity in the surround of visual cortex lesions in rats. *Neuroreport* **12**, 3341–3347.

Mittmann T, Luhmann HJ, Schmidt-Kastner R, Eysel UT, Weigel H & Heinemann U (1994). Lesion-induced transient suppression of inhibitory function in rat neocortex in vitro. *Neuroscience* **60**, 891–906.

Molnar Z & Cheung AF (2006). Towards the classification of subpopulations of layer V pyramidal projection neurons. *Neurosci Res* **55**, 105–115.

Murphy SC, Palmer LM, Nyffeler T, Muri RM & Larkum ME (2016). Transcranial magnetic stimulation (TMS) inhibits cortical dendrites. *Elife* **5**, e13598.

Ohira K, Furuta T, Hioki H, Nakamura KC, Kuramoto E, Tanaka Y, Funatsu N, Shimizu K, Oishi T, Hayashi M, Miyakawa T, Kaneko T & Nakamura S (2010). Ischemia-induced neurogenesis of neocortical layer 1 progenitor cells. *Nat Neurosci* **13**, 173–179.

Onwuekwe I & Ezeala-Adikaibe B (2012). Ischemic stroke and neuroprotection. *Ann Med Health Sci Res* **2**, 186–190.

Overman JJ, Clarkson AN, Wanner IB, Overman WT, Eckstein I, Maguire JL, Dinov ID, Toga AW & Carmichael ST (2012). A role for ephrin-A5 in axonal sprouting, recovery, and activity-dependent plasticity after stroke. *Proc Natl Acad Sci USA* **109**, E2230–2239.

Palmer LM, Schulz JM & Larkum ME (2013). Layer-specific regulation of cortical neurons by interhemispheric inhibition. *Commun Integr Biol* **6**, e23545.

Palmer LM, Schulz JM, Murphy SC, Ledergerber D, Murayama M & Larkum ME (2012). The cellular basis of GABA(B)-mediated interhemispheric inhibition. *Science* **335**, 989–993.

Pietrasanta M, Restani L & Caleo M (2012). The corpus callosum and the visual cortex: plasticity is a game for two. *Neural Plast* **2012**, 838672.

Pouille F & Scanziani M (2001). Enforcement of temporal fidelity in pyramidal cells by somatic feed-forward inhibition. *Science* **293**, 1159–1163.

Quattromani MJ, Pruvost M, Guerreiro C, Backlund F, Englund E, Aspberg A, Jaworski T, Hakon J, Ruscher K, Kaczmarek L, Vivien D & Wieloch T (2018). Extracellular matrix modulation is driven by experience-dependent plasticity during stroke recovery. *Mol Neurobiol* **55**, 2196–2213.

Reinecke S, Dinse HR, Reinke H & Witte OW (2003). Induction of bilateral plasticity in sensory cortical maps by small unilateral cortical infarcts in rats. *Eur J Neurosci* **17**, 623–627.

Rudy B, Fishell G, Lee S & Hjerling-Leffler J (2011). Three groups of interneurons account for nearly 100% of neocortical GABAergic neurons. *Dev Neurobiol* **71**, 45–61.

Schiene K, Bruehl C, Zilles K, Qu M, Hagemann G, Kraemer M & Witte OW (1996). Neuronal hyperexcitability and reduction of GABAA-receptor expression in the surround of cerebral photothrombosis. *J Cereb Blood Flow Metab* **16**, 906–914.

Schuett S, Bonhoeffer T & Hubener M (2002). Mapping retinotopic structure in mouse visual cortex with optical imaging. *J Neurosci* **22**, 6549–6559.

Shanina EV, Schallert T, Witte OW & Redecker C (2006). Behavioral recovery from unilateral photothrombotic infarcts of the forelimb sensorimotor cortex in rats: role of the contralateral cortex. *Neuroscience* **139**, 1495–1506.

Silasi G & Murphy TH (2014). Stroke and the connectome: how connectivity guides therapeutic intervention. *Neuron* **83**, 1354–1368.

Soleman S, Yip PK, Duricki DA & Moon LD (2012). Delayed treatment with chondroitinase ABC promotes sensorimotor recovery and plasticity after stroke in aged rats. *Brain* **135**, 1210–1223.

Song YM, Lee JY, Park JM, Yoon BW & Roh JK (2005). Ipsilateral hemiparesis caused by a corona radiata infarct after a previous stroke on the opposite side. *Arch Neurol* **62**, 809–811.

Takatsuru Y, Fukumoto D, Yoshitomo M, Nemoto T, Tsukada H & Nabekura J (2009). Neuronal circuit remodeling in the contralateral cortical hemisphere during functional recovery from cerebral infarction. *J Neurosci* **29**, 10081–10086.

Talelli P, Greenwood RJ & Rothwell JC (2007). Exploring Theta Burst Stimulation as an intervention to improve motor recovery in chronic stroke. *Clin Neurophysiol* **118**, 333–342.

Talelli P, Wallace A, Dileone M, Hoad D, Cheeran B, Oliver R, VandenBos M, Hammerbeck U, Barratt K, Gillini C, Musumeci G, Boudrias MH, Cloud GC, Ball J, Marsden JF, Ward NS, Di Lazzaro V, Greenwood RG & Rothwell JC (2012). Theta burst stimulation in the rehabilitation of the upper limb: a semirandomized, placebo-controlled trial in chronic stroke patients. *Neurorehabil Neural Repair* **26**, 976–987.

Wilent WB & Contreras D (2005). Stimulus-dependent changes in spike threshold enhance feature selectivity in rat barrel cortex neurons. *J Neurosci* **25**, 2983–2991.

Winship IR & Murphy TH (2008). In vivo calcium imaging reveals functional rewiring of single somatosensory neurons after stroke. *J Neurosci* **28**, 6592–6606.

Wise SP & Jones EG (1976). The organization and postnatal development of the commissural projection of the rat somatic sensory cortex. *J Comp Neurol* **168**, 313–343.

Yinon U, Chen M & Gelerstein S (1992). Binocularity and excitability loss in visual cortex cells of corpus callosum transected kittens and cats. *Brain Res Bull* **29**, 541–552.

Zhou J, Wen Y, She L, Sui YN, Liu L, Richards LJ & Poo MM (2013). Axon position within the corpus callosum determines contralateral cortical projection. *Proc Natl Acad Sci USA* **110**, E2714–2723.

Additional information

Competing interests

The authors declare that they have no competing interests.

Author contributions

BK contributed to acquisition, analysis and interpretation of data for the work, as well as drafting the work and revising it critically for important intellectual content. PM contributed to conception and design of the work and drafting the work and revising it critically for important intellectual content. We confirm that all authors approved the final version of the manuscript submitted for publication, and agree to be accountable for all aspects of the work in ensuring that questions related to the accuracy or integrity of any part of the work are appropriately investigated and resolved. All persons designated as authors qualify for authorship, and all those who qualify for authorship all listed.